VNU Journal of Science, Earth Sciences 24 (2008) 57-65

Stability of spatial interpolation functions in finite element one-dimensional kinematic wave rainfall-runoff models

Luong Tuan Anh[1,*], Rolf Larsson[2]

[1] *Research Center for Hydrology and Water Resources, Institute of Hydro-meteorological and Environmental Sciences*
[2] *Water Resources Engineering Department, Lund University, Box 118, S-221 00 Lund, Sweden*

Received 27 May 2008; received in revised form 5 July 2008

Abstract. This paper analyzes the stability of linear, lumped, quadratic, and cubic spatial interpolation functions in finite element one-dimensional kinematic wave schemes for simulation of rainfall-runoff processes. Galerkin's residual method transforms the kinematic wave partial differential equations into a system of ordinary differential equations. The stability of this system is analyzed using the definition of the norm of vectors and matrices. The stability index, or singularity of the system, is computed by the Singular Value Decomposition algorithm. The oscillation of the solution of the finite element one-dimensional kinematic wave schemes results both from the sources, and from the multiplication operator of oscillation. The results of computation experiment and analysis show the advantage and disadvantage of different types of spatial interpolation functions when FEM is applied for rainfall- runoff modeling by kinematic wave equations.

Keywords: Rainfall-runoff; Kinematic wave; Spatial interpolation functions; Singular value decomposition; Stability index.

1. Introduction

The need for tools which have capability of simulating influence of spatial distribution of rainfall and land use change on runoff processes initiated the development of hydrodynamic rainfall-runoff models [1, 8]. One of the basic assumptions for such models regards the existence of a continuous layer of water moving over the whole surface of the catchments. Although observations show that such conditions are rare, the assumption can be relaxed by considering the total flow to be the result of the flow from many small plots draining into a fine network of small channels.

The actual physical flow processes may be quite complicated, but for practical purposes there is nothing to be gained from introducing complexity into the models. As a common way of getting optimal results, the one-dimensional kinematic wave models [2, 5, 8, 11] are often selected. These can be solved by different methods, one of which is the finite element method (FEM) which is analyzed in this paper.

The FEM models are normally derived by the weighted residuals method, which is

* Corresponding author. Tel.: 84-4-917357025.
E-mail: tanh@vkttv.edu.vn

based on the principle that the solution residuals should be orthogonal to a set of weighting functions [7]:

$$\int_{\Omega} (\Re(\hat{h}) - f) W_i = 0,$$

where:

- $\Re(h) = f$: partial differential equation of h;
- $\hat{h} \approx \sum_i a_i N_i$: estimated solution;
- W_i : set of weighting functions;
- N_i : functions of spatial ordinate;
- a_i : functions of time.

According to Peyret and Taylor [9], the weighted residual method is a general and effective technique for transforming partial differential equations (PDE) into systems of ordinary differential equations (ODE). When h_i, a_i and N_i are functions defined on a spatial interval (element) the method is called FEM. The special case of weighting functions $W_i = N_i$ is called Galerkin's residual FEM and it is often used for solving one-dimensional kinematic wave rainfall-runoff models.

The numerical solutions of the finite element schemes for overland flow and groundwater flow in one dimensional kinematic wave rainfall-runoff models may often run into problems with stability and accuracy due to oscillation of the solution. The scheme may be considered stable when small disturbance are not allowed to grow in the numerical procedure. The reasons for oscillation of the Galerkin's FEM method for kinematic wave equations have been discussed by Jaber and Mohtar [5].

One important factor which influences the stability characteristics of the method is the choice of spatial interpolation function. Jaber and Mohtar [5] used linear, lumped and upwind schemes for spatial approximation and the enhanced explicit scheme for temporal discretization. They analyzed the stability of different schemes through Fourier analysis and concluded that the lumped scheme is the most suitable for solution of kinematic wave equations.

Blandford et al [2] investigated linear, quadratic, and cubic interpolation functions for simulation of one-dimensional kinematic wave by FEM and found that quadratic elements produced the most accurate solution when the implicit interaction procedure was used for temporal discretization.

The results of these researches and the mathematical implication of Galerkin's FEM show that the stability and accuracy of the finite element schemes does not only depend on the type of spatial interpolation functions, but also on the temporal integration of the system of ODE occurring when FEM is applied for overland flow kinematic wave and groundwater Boussinesq equations.

In the works cited above, the numerical schemes have been based on equi-distant spatial elements. In practical applications, it is often necessary to use elements of different size, where the discretization reflects the variation of physical properties of the channel or the catchments being modeled. The main purpose of this paper is to analyze the effects of varying size of spatial elements on the stability of the solution. Furthermore, the origin of instability will be discussed.

In the analysis, the numerical stability of the various schemes will be evaluated by investigating associated matrices using the Singular Value Decomposition (SVD) algorithm. The following types of spatial interpolation functions are investigated: linear, lumped, quadratic, and cubic.

2. Finite element schemes for one-dimensional kinematic wave equations

The one-dimensional kinematic wave

equations have been used for simulation of the rainfall-runoff process in small and average size river basins with steep slopes. They have been applied in numerous studies for hydrological design, flood forecasting etc. [2, 3, 6, 8, 11, 12]. The one-dimensional kinematic wave equations are normally written in the form of the continuity equation:

$$\frac{\partial h}{\partial t} + \frac{\partial q}{\partial x} = r(x,t)\,, \qquad (1)$$

and the equation of motion for (quasi) uniform flow:

$$q = \alpha h^{\beta}\,, \qquad (2)$$

where: h: flow depth (m); q : unit-width flow (m^2/s); $r(x,t)$: effective rainfall or lateral flow (m/s); $\alpha = S_o^{1/2}/n$; $\beta = 5/3$; n: Manning roughness coefficient ($m^{1/3}$ /s); S_o : the surface or bottom slope that equals to friction slope in the case of kinematic wave approximation; x: spatial coordinate (m); and t : time (s).

Equations (1) and (2) are partial differential equations which have no general analytical solution. However, with given initial condition $h(t=0)$ and boundary condition $h(x=0)$, numerical solutions can be found. The kinematic wave results from the changes in flow and since it is unidirectional (from upstream to downstream), only one boundary condition is required.

Principles of spatial discretization for the one-dimensional kinematic wave model using the FEM method have been presented by Ross et al [11]. The surface area of the river basin is divided in the cross-flow direction into "strips". Each strip is then divided into computational elements based on the characteristics (e.g. slope) of the basin so that each element is approximately homogeneous.

For each computational element, the variables $h(x,t)$ and $q(x,t)$ are approximated in the form:

$$h(x,t) \approx \hat{h} = \sum_{i=1}^{n} N_i(x) h_i(t); \qquad q(x,t) \approx \hat{q} = \sum_{i=1}^{n} N_i(x) q_i(t) \qquad (3)$$

where: $N_i(x)$: space interpolation function (shape function or weighting function).

It is noted that the expressions (3) should satisfy not only Equation (1) but also the initial condition and the boundary condition.

The Galerkin's residual method normalizes the approximated error with shape function over the solution domain:

$$\int_{\Omega} \sum_{i=1}^{M} \left\{ \frac{dh_i}{dt} N_i + q_i \frac{\partial N_i}{\partial x} - r_i \right\} N_i dx = 0\,. \qquad (4)$$

The approximation (3) combined with the integral (4) transforms the partial differential Equation (1) into a system of ordinary differential equations, which for each element (4) takes the form:

$$A^{(e)} \frac{dh}{dt} + B^{(e)} q - f^{(e)} = 0\,. \qquad (5)$$

For the linear scheme, the spatial interpolation functions can be defined as:

$N_1(x) = 1 - y$, and $N_2(x) = y$,

where $y = x/l$; l is the length of the element.

In this case, the matrices of Equation (5) are written as:

$$\mathbf{B}^{(e)} = \frac{1}{2}\begin{bmatrix} -1 & 1 \\ -1 & 1 \end{bmatrix};$$

$$\mathbf{A}^{(e)} = \begin{bmatrix} \frac{l}{3} & \frac{l}{6} \\ \frac{l}{6} & \frac{l}{3} \end{bmatrix}; \quad \mathbf{f}^{(e)} = \begin{bmatrix} \frac{l}{2} \\ \frac{l}{2} \end{bmatrix} r(x,t)$$

The lumped scheme [5] is based on the spatial interpolation functions expressed in the forms:

$$N_{j-1}^{*} = 1 - H\left(s - \frac{l}{2}\right); \; N_j^{*} = H\left(s - \frac{l}{2}\right)$$

The heavyside function $H(x)$ is defined as:

$H(x) = 0$ if $x < 0$;

$H(x) = 1$ if $x \geq 0$;

s: distance from node j-1.

The matrices for the lumped scheme of Equation (5) can be estimated in the form:

$$\mathbf{A}^{(e)} = \frac{1}{2}\begin{bmatrix} l & 0 \\ 0 & l \end{bmatrix}$$

The matrix $\mathbf{B}^{(e)}$ and vector $\mathbf{f}^{(e)}$ remain the same as linear scheme.

In the case of quadratic scheme [2], the spatial interpolation functions are:

$$N_1 = 1 - 3y + 2y^2;$$

$$N_2 = 4y - 4y^2;$$

$$N_3 = -y + 2y^2.$$

The matrices for one element are defined as following:

$$\mathbf{A}^{(e)} = \begin{bmatrix} \frac{2l}{15} & \frac{l}{15} & -\frac{l}{30} \\ \frac{l}{15} & \frac{8l}{15} & \frac{l}{15} \\ -\frac{l}{30} & \frac{l}{15} & \frac{2l}{15} \end{bmatrix};$$

$$\mathbf{B}^{(e)} = \begin{bmatrix} -\frac{1}{2} & \frac{2}{3} & -\frac{1}{6} \\ -\frac{2}{3} & 0 & \frac{2}{3} \\ \frac{1}{6} & -\frac{2}{3} & \frac{1}{2} \end{bmatrix}; \quad \mathbf{f}^{(e)} = \begin{bmatrix} \frac{l}{6} \\ \frac{2l}{3} \\ \frac{l}{6} \end{bmatrix} r(x,t)$$

For cubic scheme (one element, four nodes), spatial interpolation functions can be expressed in the forms:

$$N_1 = 1 - 5.5y + 9y^2 - 4.5y^3$$

$$N_2 = 9y - 22.5y^2 + 13.5y^3$$

$$N_3 = -4.5y + 18y^2 - 13.5y^3$$

$$N_4 = y - 4.5y^2 + 4.5y^3$$

The matrices for one element are integrated and are presented as:

$$\mathbf{A}^{(e)} = \begin{bmatrix} \frac{8}{105}l & \frac{33}{560}l & -\frac{3}{140}l & \frac{19}{1680}l \\ \frac{33}{560}l & \frac{27}{70}l & -\frac{27}{560}l & -\frac{3}{140}l \\ -\frac{3}{140}l & -\frac{27}{560}l & \frac{27}{70}l & \frac{33}{560}l \\ \frac{19}{1680}l & -\frac{3}{140}l & \frac{33}{560}l & \frac{8}{105}l \end{bmatrix};$$

$$\mathbf{B}^{(e)} = \begin{bmatrix} -\frac{1}{2} & \frac{57}{80} & -\frac{3}{10} & \frac{7}{80} \\ -\frac{57}{80} & 0 & \frac{81}{80} & -\frac{3}{10} \\ \frac{3}{10} & -\frac{81}{80} & 0 & \frac{57}{80} \\ -\frac{7}{80} & \frac{3}{10} & -\frac{57}{80} & \frac{1}{2} \end{bmatrix}; \quad \mathbf{f}^{(e)} = \begin{bmatrix} \frac{l}{8} \\ \frac{3l}{8} \\ \frac{3l}{8} \\ \frac{l}{8} \end{bmatrix} r(x,t)$$

For the whole domain containing the elements, Equation (5) has the form:

$$\mathbf{A}\frac{d\mathbf{h}}{dt} + \mathbf{B}\mathbf{q} - \mathbf{f} = 0 \tag{6}$$

In the case of using lumped scheme, matrices **A**; **B** and vector **f** for the domain (strip) containing n elements can be presented in the forms:

$$\boldsymbol{A} = \begin{bmatrix} \frac{l_1}{2} & 0 & 0 & 0 & 0 & . & . & . & 0 & 0 \\ 0 & \frac{l_1}{2}+\frac{l_2}{2} & 0 & 0 & 0 & 0 & . & . & 0 & 0 \\ 0 & 0 & \frac{l_2}{2}+\frac{l_3}{2} & 0 & 0 & 0 & . & . & 0 & 0 \\ 0 & 0 & 0 & \frac{l_3}{2}+\frac{l_4}{2} & 0 & 0 & 0 & . & . & 0 \\ 0 & 0 & 0 & 0 & \frac{l_4}{2}+\frac{l_5}{2} & 0 & 0 & . & . & 0 \\ 0 & 0 & 0 & 0 & 0 & \frac{l_5}{2}+\frac{l_6}{2} & 0 & . & . & 0 \\ . & . & . & . & . & . & . & . & . & . \\ 0 & 0 & 0 & . & . & 0 & 0 & \frac{l_{n-2}}{2}+\frac{l_{n-1}}{2} & 0 & 0 \\ 0 & 0 & 0 & 0 & . & . & 0 & 0 & \frac{l_{n-1}}{2}+\frac{l_n}{2} & 0 \\ 0 & 0 & 0 & 0 & . & . & 0 & 0 & 0 & \frac{l_n}{2} \end{bmatrix}.$$

$$\boldsymbol{B} = \begin{bmatrix} -\frac{1}{2} & \frac{1}{2} & 0 & 0 & 0 & . & . & . & 0 & 0 \\ -\frac{1}{2} & 0 & \frac{1}{2} & 0 & 0 & . & . & . & 0 & 0 \\ 0 & -\frac{1}{2} & 0 & \frac{1}{2} & 0 & 0 & . & . & 0 & 0 \\ 0 & 0 & -\frac{1}{2} & 0 & \frac{1}{2} & 0 & 0 & . & . & 0 \\ 0 & 0 & 0 & -\frac{1}{2} & 0 & \frac{1}{2} & 0 & . & . & 0 \\ . & . & . & . & . & . & . & . & . & . \\ . & . & . & . & . & . & . & . & . & . \\ 0 & 0 & . & . & 0 & 0 & -\frac{1}{2} & 0 & \frac{1}{2} & 0 \\ 0 & 0 & . & . & . & 0 & 0 & -\frac{1}{2} & 0 & \frac{1}{2} \\ 0 & 0 & . & . & . & 0 & 0 & 0 & -\frac{1}{2} & \frac{1}{2} \end{bmatrix}$$

$$\mathbf{f} = \begin{bmatrix} \frac{l_1 r_1}{2} \\ \frac{l_1 r_1}{2} + \frac{l_2 r_2}{2} \\ \frac{l_2 r_2}{2} + \frac{l_3 r_3}{2} \\ \cdot \\ \cdot \\ \cdot \\ \frac{l_{n-1} r_{n-1}}{2} + \frac{l_n r_n}{2} \\ \frac{l_n r_n}{2} \end{bmatrix} = \mathbf{Cr}$$

For overland flow, the system of ordinary differential equations (6), can be written in the form:

$$\mathbf{A}\frac{d\mathbf{h}}{dt} + \mathbf{Bq} - \mathbf{Cr} = 0, \qquad (7)$$

where: **C**: sparse matrix containing the size of elements; **r**: vector of effective rainfall.

The solution of Equation (7) can be obtained by various numerical methods, one of which is the standard Runge-Kutta method and Successive Linear Interpolation for solution of ODE with boundaries [4, 10].

In order to analyze how the stability and accuracy of the solution schemes depends on the choice of spatial interpolation functions, equation (7) has been transformed into a system of linear algebraic equations:

$$\mathbf{Ax} = \mathbf{y}, \qquad (8)$$

where: $\frac{\Delta\mathbf{h}}{\Delta t} = \mathbf{x}$: unknown vector;

$\mathbf{y} = \mathbf{Cr} - \mathbf{Bq}$: given vector for explicit temporal differential scheme and estimated vector for implicit interactive scheme for each time step.

3. Stability and error analysis

In order to evaluate the stability of various finite element schemes, the Singular Value Decomposition (SVD) algorithm will be applied. It will be introduced and described below together with the definition of some essential vector and matrix concepts:

(i) According to the SVD algorithm [4. 10], the matrix A (m×m) can be expressed in the form:

$$\mathbf{A} = \mathbf{U}\Sigma\mathbf{V}^T, \qquad (9)$$

where **U**, **V**: square orthogonal matrices (m×m), $\mathbf{\Sigma}$: diagonal matrix with $\delta_{ii} \neq 0$ called singular values of matrix A.

(ii) The norm of the vector **x** is defined as:

$$\|\mathbf{x}\| = (\mathbf{x}^T \bullet \mathbf{x})^{1/2} \qquad (10)$$

(iii) The norm of the matrix A is defined as the maximum coefficient of extension and can be expressed as:

$$\|\mathbf{A}\| = \|\mathbf{U}\,\Sigma\,\mathbf{V}^T\| \le \|\mathbf{U}\|\|\Sigma\|\|\mathbf{V}^T\| = \|\Sigma\| = \delta_{\max} \qquad (11)$$

The physical implication of Equation (8) is that one vector, x, in linear space is transformed by **A** into another vector, y. This transformation takes three different forms: extension, compression, and turning.

The stability index, or singularity of the matrix **A**, can be defined as the ratio of maximum extension capacity over the minimum compression capacity, expressed as [4]:

$$Cond(A) = \frac{\max\limits_x \frac{\|Ax\|}{\|x\|}}{\min\limits_x \frac{\|Ax\|}{\|x\|}} = \frac{\max\limits_x \frac{\|U\Sigma V^T x\|}{\|x\|}}{\min\limits_x \frac{\|U\Sigma V^T x\|}{\|x\|}} = \frac{\delta_{\max}}{\delta_{\min}}, \qquad (12)$$

where $\delta_{\max}, \delta_{\min}$: maximum and minimum singular values of **A** respectively.

Now, in order to study the stability of the solution scheme, a disturbance (oscillation) Δy is introduced. This results in a corresponding disturbance (oscillation) Δx in the solution. The system of linear algebraic equations (8) with and without oscillation becomes:

$$\mathbf{Ax} = \mathbf{y} \;\Rightarrow\; \|\mathbf{y}\| \le \|\mathbf{A}\| \bullet \|\mathbf{x}\| = \delta_{\max}\|\mathbf{x}\| \qquad (13)$$

$$\mathbf{A}(\mathbf{x} + \Delta\mathbf{x}) = \mathbf{y} + \Delta\mathbf{y} \;\Rightarrow\; \|\Delta\mathbf{y}\| \ge \delta_{\min}\|\Delta\mathbf{x}\|,$$

where: $\Delta\boldsymbol{x}, \Delta\boldsymbol{y}$: oscillation vector of solution and oscillation vector of errors respectively.

This means that:

$$\frac{\|\Delta\mathbf{x}\|}{\|\mathbf{x}\|} \le Cond(\mathbf{A})\frac{\|\Delta\mathbf{y}\|}{\|\mathbf{y}\|} \qquad (14)$$

The relationship (14) shows that the stability of the solution of system (8) depends on the stability index of the matrix **A** with a high value of the index indicating lower stability. The relationship (14) also means that the stability index (or singularity of **A**) may be considered as the multiplication of oscillation $\mathbf{\Delta y}$:

$$\mathbf{\Delta y} = \mathbf{C\Delta r} - \mathbf{B\Delta q}. \tag{15}$$

The upper limit of oscillation (15) can be estimated by applying the definition of the norm of vectors and matrices:

$$\begin{aligned} \|\boldsymbol{\Delta y}\| &= \|\boldsymbol{C}\Delta\boldsymbol{r} - \boldsymbol{B}\Delta\boldsymbol{q}\| \leq \\ &\leq \|\boldsymbol{C}\Delta\boldsymbol{r}\| + \|\boldsymbol{B}\Delta\boldsymbol{q}\| \leq \delta^C_{\max}\|\Delta\boldsymbol{r}\| + \delta^B_{\max}\|\Delta\boldsymbol{q}\| \end{aligned} \tag{16}$$

where: $\delta^B_{\max}$: maximum singular value of matrix **B**; $\delta^C_{\max}$: maximum singular value of matrix **C**.

Expression (16) shows that the source of oscillation include oscillation in the source term $\boldsymbol{r}$ (effective rainfall) as well as oscillation in the advection term accumulated during the computation process. The upper limits of these oscillations depend on the chosen spatial interpolation function, and they are related with the structure of the matrices **B** and **C** respectively. These values will be computed and the results will be discussed below for the selected types of interpolation functions.

The solution of the system (8) normally requires to inverse matrix **A** [5, 12]. We can show that the singularity of the (square) matrix **A** has the same value as the singularity of the inverse matrix $\mathbf{A}^{-1}$ by using Equation (9):

$$\mathbf{A}^{-1} = \mathbf{V\Sigma}^{-1}\mathbf{U}^T. \tag{17}$$

Application of Singular Value Decomposition of $\mathbf{A}^{-1}$ gives:

$$\mathbf{A}^{-1} = \mathbf{U}'\mathbf{\Sigma}'\mathbf{V}'^T. \tag{18}$$

The decompositions (9) and (18) are "almost" unique [10]. It means that $\Sigma^{-1} = \Sigma'$, and:

$$\begin{aligned} Cond(A) &= \frac{\delta_{\max}}{\delta_{\min}} = Cond(A^{-1}) = \\ &= \left(\frac{1}{\delta_{\min}}\right) / \left(\frac{1}{\delta_{\max}}\right) \end{aligned} \tag{19}$$

The relationships (14) and (19) show that the stability and accuracy of solution of system (8) are directly related with the singularity of the hard matrix **A**.

4. Numerical experiments

In order to verify the methodology, some basic investigations are made for different types of interpolation schemes in section 4.1. In section 4.2, the effect of using elements of various lengths is investigated. Finally, in section 4.3, the influence of different disturbance sources is analyzed.

4.1. Stability index of matrix A for different types of spatial interpolation functions

Now we assume that the studied strip of surface area is divided into elements of (equal) unit length. The index of stability of matrix **A** has been computed for various numbers of elements for each type of interpolation function. The results of the computations are presented in Fig. 1.

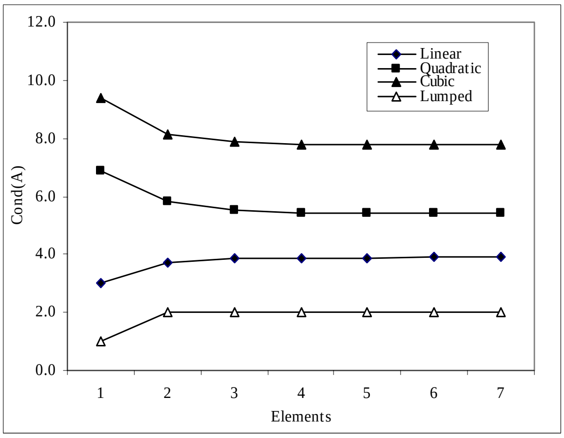

Fig. 1. The change of stability index of matrix **A**.

The numerical experiments show that the index of stability is virtually constant for each type of interpolation scheme when the number of elements is two or higher. It is also clear that the lumped scheme gives the lowest value of stability index, while linear, quadratic and cubic schemes give 2, 3 and 4 times higher values respectively. In conclusion, the lumped scheme has the highest order of stability among the four studied numerical schemes.

The results of numerical experiments presented above agree well with the results of analytical Fourier stability analysis for consistent (linear) and lumped schemes that have been presented in the work by Jaber and Mohtar [5].

4.2. The impact of finite element approximations

Numerical experiments have been conducted in order to assess the effect of element size on stability of the four finite element schemes: linear, lumped, quadratic and cubic. The calculations have been made for a strip of 1000 m length, which has been approximated by two elements. The lengths of the two elements have been chosen according to three different options, with more or less asymmetric proportions: option 1 with proportions 1:1, option 2 with proportions 1:9, and option 3 with proportions 1:99.

The stability index of matrix **A** and the maximum extension capacity of errors of matrices **B** and **C** have been computed and are shown in Table 1. The results show that the stability of the finite element one-dimensional kinematic wave schemes does not only depend on the type of spatial interpolation function, but also on the spatial discretization of the surface strip considered. For all four interpolation schemes, the lower the stability is, the more disproportionate the elements are. At the same time for all three options, each with different geometric proportions, the stability is higher for lumped and linear schemes than that for quadratic and cubic schemes.

Another conclusion is that there are two main causes for oscillation of the solution. One is the oscillation sources, and the other one is the multiplication operator. Furthermore, it should be pointed out that the efficiency of the algorithm is an important aspect with regards to the choice of interpolation scheme for practical applications. The linear and lumped schemes require n+1 equations, while quadratic and cubic schemes require 2n+1 and 3n+1 equations respectively for solving a problem with n elements.

Table 1. Stability index of matrix **A** and maximum coefficient of oscillation

Cases of study		Linear	Lum-ped	Quad-ratic	Cubic
Option 1	$\delta^B_{\max}$	0.866	0.866	1.29	1.67
	$\delta^C_{\max}$	404.5	404.5	334.2	198.7
	Cond (A)	3.73	2.00	5.83	8.13
Option 2	$\delta^B_{\max}$	0.866	0.866	1.29	1.67
	$\delta^C_{\max}$	452.8	452.8	618.5	355.8
	Cond (A)	14.6	10.0	41.2	63.1
Option 3	$\delta^B_{\max}$	0.866	0.866	1.29	1.67
	$\delta^C_{\max}$	495.0	495.0	680.3	391.3
	Cond (A)	149.6	100.0	448.8	688.6

4.3. The upper limit of oscillation sources for different types of spatial interpolation functions

If the oscillation occurring at a given time step are supposed to be equal for different types of spatial functions, then the upper limit of source of oscillation will be related with the maximum singular values of matrices **B** and **C**. The structure of these matrices is depended on the type of interpolation functions. The maximum singular values of **B** and **C** for unit elements of equal length have been computed and are presented in Table 2.

The results show that for advection oscillation, both the linear and the lumped schemes give values that are nearly independent of the number of elements, while the quadratic and cubic schemes exhibit increasing values for increasing number of elements (see Fig. 2). The experiment also shows that linear and lumped schemes have the same source of oscillation. They can also control the advection oscillation better than quadratic and cubic ones. However, the oscillation of effective rainfall component is better controlled by quadratic and cubic schemes than by lumped and linear ones.

Table 2. Maximum coefficients of source of oscillation

Number of elements	Para-meters	Linear	Lum-ped	Quad-ratic	Cubic
1	$\delta^B_{\max}$	1.0	1.0	1.16	1.55
	$\delta^C_{\max}$	0.500	0.500	0.667	0.375
2	$\delta^B_{\max}$	0.866	0.866	1.29	1.67
	$\delta^C_{\max}$	0.809	0.809	0.689	0.398
3	$\delta^B_{\max}$	1.0	1.0	1.33	1.71
	$\delta^C_{\max}$	0.901	0.901	0.689	0.398
4	$\delta^B_{\max}$	0.951	0.951	1.34	1.73
	$\delta^C_{\max}$	0.940	0.940	0.689	0.398
5	$\delta^B_{\max}$	1.0	1.0	1.35	1.74
	$\delta^C_{\max}$	0.960	0.960	0.689	0.398
6	$\delta^B_{\max}$	0.975	0.975	1.35	1.75
	$\delta^C_{\max}$	0.971	0.971	0.689	0.398
7	$\delta^B_{\max}$	1.0	1.0	1.35	1.75
	$\delta^C_{\max}$	0.978	0.978	0.689	0.398

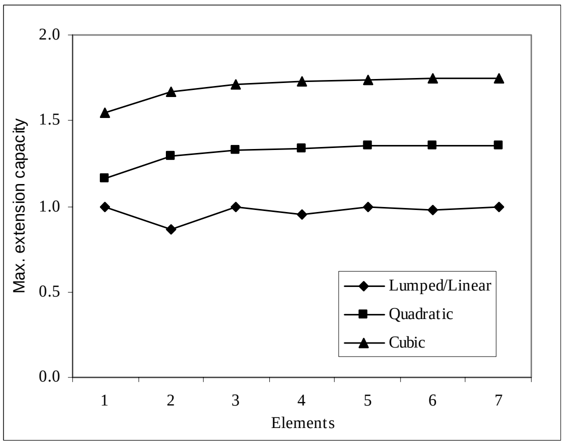

Fig. 2. The change of maximum extension capacity of matrix **B**.

5. Conclusions

This paper analyses the sources and causes of oscillation of solutions for finite element one dimensional rainfall-runoff models when different types of spatial interpolation functions is applied for overland flow kinematic wave simulation. It does so by applying the definition of norm of vectors and matrices and the Singular Value Decomposition (SVD) algorithm.

The structure of matrix **A**, which contains sizes of the finite elements, is related to the type of spatial interpolation function which is applied. From the above presented results and discussions, it can be concluded that the stability index or singularity of matrix **A** can be considered as an effect of multiplication of oscillation occurring during computation process. It will affect the stability and accuracy of the solution of finite element one-dimensional kinematic wave schemes, and it is actually one of the main causes of oscillation of solutions.

The results of computation experiment show the advantage and disadvantage of different types of spatial interpolation functions when FEM is applied for rainfall-runoff kinematic wave models. If the reason for growing oscillation is seen as the most important criterion for assessing stability of numerical schemes, the lumped and linear schemes have higher order of stability than the quadratic and cubic schemes. However, when the lumped scheme is used, the matrix **A** becomes a diagonal matrix and then the algorithm is more efficient than all other three types of schemes.

The results also show that the finite element one-dimensional kinematic wave schemes can be improved by choosing the most suitable spatial interpolation function for decreasing the singularity of matrix **A** and minimize the source of oscillation. The spatial interpolation functions of higher order do not always give improved results when finite element method is used for kinematic wave rainfall-runoff models.

References

[1] M.B. Abbott, J.C. Bathurst, J.A. Cunge, P.E. O' Connel, J. Rasmussen, Structure of a physically-based distributed modeling system, *J. Hydrol.* 87 (1986) 61.

[2] G.E. Blandford, M.E. Meadows, Finite element simulation of nonlinear kinematic surface runoff. *J. Hydrol.* 119 (1990) 335.

[3] V.T. Chow, D.R. Maidment, L.W. Mays, *Applied hydrology*, Mc Graw Hill Book Company, 1998.

[4] G.E. Forsythe, M.A. Malcolm, C.B. Moler, *Computer method for mathematical computations*, Prentice-Hall, New Jersey, USA, 1977.

[5] F.H. Jaber, R.H. Mohtar, Stability and accuracy of finite element schemes for the one-dimensional kinematic wave solution, *Adv. Water Resource* 25 (2002) 427.

[6] R.S. Kurothe, N.K. Goel, B.S. Mathur, Derivation of a curve number and kinematic wave based flood frequency distribution, *Hydrol. Sci. J.* 46 (2001) 571

[7] C.G. Koutitas, *Element of computational hydraulics*, Pentech Press, London: Plymouth, 1983.

[8] L.S. Kuchment, *Mathematical modeling of river flow formulation processes*, Hydromet. Book, Russia, 1980.

[9] R. Peyret, T.D. Taylor, *Computational methods for fluid flow*, Springer-Verlag, USA, 1983.

[10] W. Press, S. Teukolsky, W. Vetterling, B. Flannery, *Numerical recipes in Fortran*, The Art of Scientific Computing, Second edition, Cambridge University Press, 1992.

[11] B.B. Ross, D.N. Contractor, V.O. Shanholtz, Finite element model of overland and channel flow for assessing the hydrologic impact of land use change, *J. Hydrol.* 41 (1979) 11.

[12] Y. Yuyama, *Regional drainage analysis by mathematical model simulation,* National Research Institute of Agricultural Engineering, Japan, 1996.